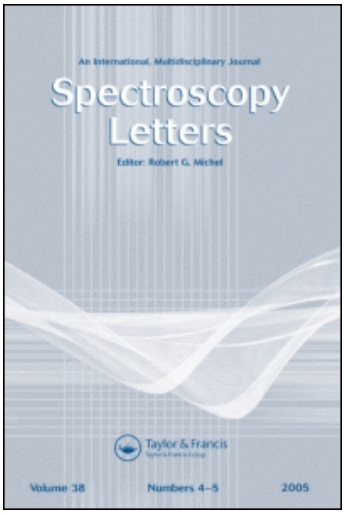

Spectroscopy Letters
Publication details, including instructions for authors and subscription information:
http://www.informaworld.com/smpp/title~content=t713597299

Stimulated Raman Scattering in Hydrogen Using Capilary Cell

H. Bryant[a]; K. Sentrayan[a]; V. Kushawaha[a]
[a] Laser Physics Laboratory, Department of Physics, Howard University, Washington, D.C.

To cite this Article Bryant, H. , Sentrayan, K. and Kushawaha, V.(1992) 'Stimulated Raman Scattering in Hydrogen Using Capilary Cell', Spectroscopy Letters, 25: 8, 1387 — 1403
To link to this Article: DOI: 10.1080/00387019208017871
URL: http://dx.doi.org/10.1080/00387019208017871

SPECTROSCOPY LETTERS, 25(8), 1387-1403 (1992)

STIMULATED RAMAN SCATTERING IN HYDROGEN USING CAPILARY CELL

Key Words: Laser, H_2, Raman–Scattering, Stokes, anti–Stokes

H. Bryant, K. Sentrayan, and V. Kushawaha
Laser Physics Laboratory, Department of Physics
Howard University, Washington, D.C. 20059

ABSTRACT

Stimulated Raman Scattering processes have been studied and intense Stokes and anti–Stokes laser lines have been observed in a capillary Raman cell filled with molecular hydrogen and pumped by the third harmonic of the Nd:YAG laser at wavelength $\lambda = 355$ nm. Various parametric studies have been performed to establish an optimum condition for the best operation of the Raman laser. The observation of higher–order Stokes and anti–Stokes has been explained on the basis of four–wave mixing and/or cascade energy transfer processes.

Introduction

The Stimulated Raman Scattering (SRS) is an attractive technique for the generation of highly coherent new laser lines in a Raman gain medium pumped by a high energy pulsed laser beam. This technique has been extensively used in gaseous media such as H_2, D_2, and CH_4, etc. pumped by either a single laser line such as Nd:YAG (fundamental and its harmonics) and excimer lasers or tunable dye lasers and Raman laser lines (Stokes and anti–Stokes lines) at different wavelengths have been observed by many

investigators in the past [1–6]. The SRS is a non–linear two–photon process and requires very high power input laser beam. At high power density (in GW/cm^2 range), the gaseous breakdown of the molecular species and the Brillouin scattering are the major problems and may be responsible for low conversion efficiency of the Raman laser lines. The Brillouin scattering may be avoided by using a pump laser of short pulse duration whereas the gaseous breakdown may be avoided by using a longer Raman cell (> 1 meter). Most of the previous studies have used long Raman cells of wider (>1" diameter) to study the SRS–processes. The diameter of the laser beam used by most of the investigators in the past range from 5 to 6 mm and therefore all the molecules in the Raman cell of diameter 1" or more do not interact with the laser beam and thus do not participate in the SRS–processes. Some experiments have been performed by using multiple–pass [7–8] Raman cell which increases the interaction of the pump laser photons and molecules within the cell and thereby increasing the efficiency of the Raman laser lines. However, the whole device becomes too complicated and bulky in this configuration and therefore of less practical use.

In this communication, we report our observations on the formation of the Stokes frequency at ($\nu_{s_n} = \nu_p - n\ \nu_r$) and anti–Stokes frequency ($\nu_{as_n} = \nu_p + n\ \nu_r$) in H_2 gas in a capillary Raman cell pumped by the third harmonic of the Nd:YAG laser at wavelength $\lambda = 355$ nm. Here ν_{s_n} and ν_{as_n} are the Stokes and anti–Stokes frequencies, ν_p and ν_r are the laser pump and Raman transition frequencies, respectively, and n is an integer. For H_2 molecule, $\nu_r = 4155$ cm^{-1}. In addition to our main objective of studying the SRS–processes in a capillary tubing, the first and second Stokes lines at $\lambda = 416$ and 503 nm, respectively, may be used for laser submarine communication [9] and the first anti–Stokes line at $\lambda = 274$ nm may be used for measuring the atmospheric O_3 concentration [10–13] using LIDAR (LIght Detection And Ranging) techniques. The experimental details and the results obtained will be described below.

Experimental Details

The experimental set–up used to study the Raman scattering processes is shown in Fig. 1. It consists of a Raman cell, pulsed laser, and optical detection

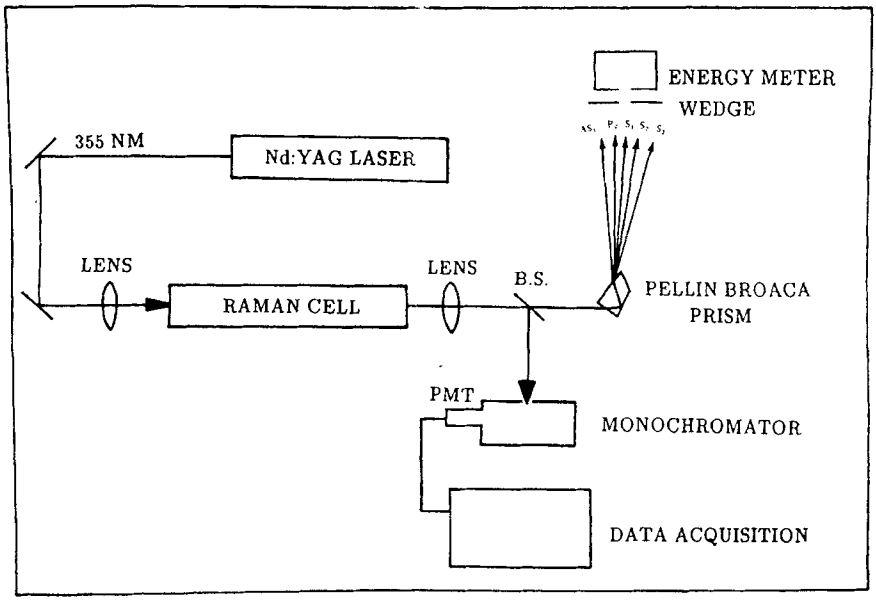

Fig.1 Schematic diagram of the experimental set–up used to study the SRS–processes in H_2–gas. The notations P_0, S_1, S_2, S_3 and AS_1 are the pump, first, second, third, and first anti–Stokes, respectively. B.S = Beam splitter and PMT = Photomultiplier tube.

system. The Raman cell was made of stainless steel, 40 cm long and 0.635 cm in diameter. For better handling and ease of operation of this cell, the 0.635 cm diameter tubing was welded with another stainless tubing of 2.54 cm diameter and 40 cm in length. Two additional tubings 0.635 cm in diameter and about 15 cm long were also attached to the larger diameter tubing only in a direction perpendicular to the optical axis of the Raman cell. One of these tubings, located on one end of the Raman cell was connected to the H_2 gas tank with a single stage gas regulator and a valve for controlled delivery of H_2–gas into the Raman cell. The other tubing, located on the other end of the Raman cell, was used to measure the gas–pressure inside the Raman cell. The pressure gauge was calibrated and capable of reading gas pressure in

the range of 0 – 1000 PSI (14.7 PSI = 1 Atmosphere). The two ends of the Raman cell were shielded with 0.635 thick and 2.54 cm diameter quartz windows. It is to be noted here that a window of this thickness was necessary to sustain the high gas pressure inside the Raman cell. These two windows were supported by a pair of Viton O–rings. For the ease of operation, the entire Raman cell assembly was put in a set of two annular metal rings with adjustable screws. The H_2 gas used in the present study was of high purity (99.999%), purchased from Air–Products, and was used without further purification.

The Raman Scattering processes were studied by pumping the H_2 gas using the third harmonic of the Nd:YAG laser at wavelength λ = 355 nm (Lumonics model HY–500). The laser beam was directed into the Raman cell by using a set of steering mirrors coated for high reflectivity (99.5%) and high damage threshold (10 GW/cm^2) at the pump wavelength λ = 355 nm. The directed beam was then focused into the Raman cell by means of a quartz lens of 50 cm focal length. The focal point inside the Raman cell was adjusted to be at the center of the cell.

The output beam from the Raman cell consisted of the main beam, i.e., the pump laser beam (355 nm) and other Raman components, i.e., Stokes and anti–Stokes laser lines due to Raman scattering in H_2 gas. The output beam in the forward direction was collimated by another lens of 40 cm focal length. The collimated beam was then split–off by a quartz plate which reflected about 4% of the total beam energy. The reflected beam was dispersed by a 0.2m scanning monochromator (McPherson model 275 and stepping motor controller model 789) and detected by a photomultiplier tube (PMT) (EMI–Gen Com model–9863QB/5) at room temperature. The spectrum was scanned in the wavelength range of 300–644 nm and the output from the PMT was amplified and sent to a multichannel analyzer (MCA) (Norland corporation model–480). The output from the MCA was plotted on an X–Y chart recorder for future use. The rest of the 96% of the forward collimated beam was dispersed by a set of two Pellin–Broca prisms made of BK7 glass. A white target at about 20–feet was used to display the dispersed laser beams, pump as well as the Raman components (Stokes and anti–Stokes). The energy of the pump laser beam and the Raman components was

measured by a calibrated energy meter (Sci-tech model 362). For the energy measurement of the depleted pump beam, i.e., 355 nm laser beam and the Raman components, i.e., Stokes and anti–Stokes beams, it was necessary to use a wedge to isolate the unwanted components and pass only the a particular component of interest.

A parametric study on the generation of the Raman components was done by varying the H_2–gas pressure in the range of 200–500 PSI, laser beam energy in the range of 1–60 mJ and focal point of the focusing lens inside the Raman cell. The results obtained will be described below.

Results and Discussions

As noted above, the gaseous breakdown is a major problem at very high intensity of the pump laser beam in gaseous Raman gain media. For the non–linear SRS–processes to occur, a high laser beam intensity is required. To study the Raman processes and avoid the gaseous breakdown at the same time, most of the previous studies have used longer than or at least 1–meter long Raman cell(s) with internal diameter of 1–inch or more. We decided to decrease the length of the Raman cell to 40 cm keeping the internal diameter to 1–inch and studied the Raman processes at a reasonably high H_2–gas pressure and laser beam intensity of about 30 mJ. Under these conditions, we were unable to observe any scattered laser light. An attempt to observe these colors, we placed another identical Raman cell in tandem configuration and pumped both the cells with the same 355 nm laser beam at about 30 mJ. However, there was no success in observing the expected scattered laser beams. It is to be noted here that the diameter of the collimated laser beam used here is about 5–6 mm. This means that the laser beam is interacting only with those molecules which are in the laser beam cylinder and rest of the H_2 molecules are not being utilized in the scattering processes. Because of this reason, we decided to change the configuration of the Raman cell by narrowing the Raman cell diameter and to make it act like a waveguide. For this purpose, we fabricated a Raman cell of 40 cm in length and 0.635 cm (= 1/4") in internal diameter forming a laser cylinder of volume $\{(\pi r^2 L = 3.14 \times (0.635/2)^2 \times 40\}$ cm^3.

In this configuration the number density of the H_2 molecules would be 16 times more as compared to $\{3.14x(2.54/2)^2x40\}$ cm^3 with 1" internal diameter. When the newly designed Raman cell was pressurized to a pressure of $\cong$ 350 PSI of H_2 gas and pumped by the laser beam of wavelength λ = 355 nm and $\cong$ 30 mJ of energy focused to a beam diameter of $\cong$ 1mm, bright colors of violet, green, and red were observed. The results obtained at different experimental conditions using the capillary Raman cell will be described below.

A: Laser Beam Energy Dependence on the SRS–Processes

The laser beam intensity dependence on the forward SRS–processes was studied in the energy range of 1–60 mJ (pulse duration 8 nsec) and at a constant H_2–gas pressure of 500 PSI at room temperature. The focal spot size of the laser beam inside the Raman cell was about 1 mm leading to the power density of $\cong$ $(16–955)x10^6$ W/cm^2. The initial sign of the SRS–processes was realized when the laser beam intensity was $\cong$ 1 mJ. This was evident due to the weak appearance of a blue spot on the screen located at about 20' away from the Raman cell. This observation is consistent with the energy threshold observed by Komine et al [14]. When the laser beam energy was slightly increased to about 3 mJ, the violet (λ = 416 nm, first Stokes) became intense, the green (λ = 503 nm, second Stokes) was intermittent and the red (λ = 636 nm, third Stokes) was absent. At pulsed energy of about 13 mJ, the violet and green colors became very bright and the red color was intermittent which became bright when the pulsed energy was increased to 20 mJ. As mentioned earlier that part of the collimated beam was sent to the scanning monochromator and detected by a room temperature PMT and rest of the scattered beam was dispersed by a BK–7 glass Pellin–Broca prism. Because of the absorbing nature of the glass for radiation shorter than $\cong$ 300 nm, it was not possible to observe the shorter wavelengths, anti–Stokes laser lines, even if they were being generated inside the Raman cell due to the SRS–processes. However, indirect evidence is available to show that the high order anti–Stokes lines were produced at higher energies of the pump laser beam. In Fig. 2, we display the wavelength scan with relative

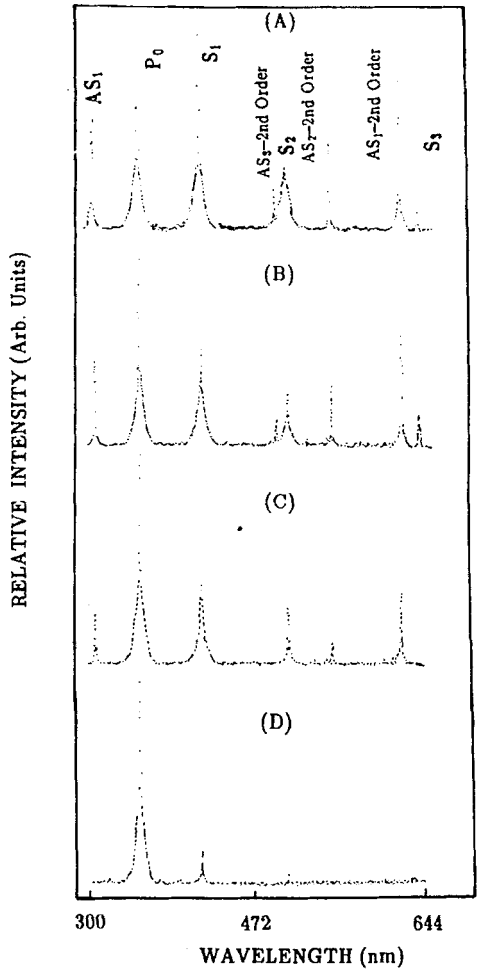

Fig. 2 Wavelength scan of the Raman components with pump laser beam energies at H_2–gas pressure = 500 PSI and focal point = 20 cm. The spectra are not corrected for the spectral response of the optical detection system. A: 50 mJ, B: 13 mJ, C: 10 mJ, D: 3.6 mJ. The notations are the same as in Fig. 1.

intensity of the Raman components at a few selected input energies in the wavelength range of 300–664 nm. It is clear from this figure that the second–order of the first, second, and third anti–Stokes Raman lines are present at higher laser beam energies indicating that the first–order anti–Stokes lines at λ = 309 nm, 274 nm, and 246 nm are being generated in the SRS–processes in the I_2 gas. In addition to the generation of the first, second, and third Stokes and anti–Stokes laser lines, it is possible that the fourth Stokes and anti–Stokes line may have been present at high laser energies but could not be recorded mainly due to the limitation imposed by the optical detection system in the present study. The efficiency of the PMT used to detect these emission lines is very poor beyond the wavelength range of 300–700 nm. The fourth Stokes and anti–Stokes lines are expected to appear at λ = 864 nm and λ = 223 nm, respectively. It is to be noted here that if the fourth anti–Stokes line (λ=223 nm) was being produced at higher laser energy (60 mJ is the highest energy used in the present study), the second–order should have been observed at λ = 446 nm. A close inspection of Fig. 2 indicates that indeed there is a trace of this line at around 446 nm. Because of the weak nature of this line, the 60 mJ may be regarded as the threshold for the observation of the fourth anti–Stokes line and its intensity is expected to grow as the laser beam energy is further increased beyond 60 mJ. Based on this observation, it may be concluded that the fourth Stokes line is also being produced at higher energies ($\gtrsim$ 60 mJ or more) but could not be recorded in the present study. It is also to be noted here that the intensity of the Stokes lines are always higher than the anti–Stoke lines and therefore the intensity of the fourth Stokes lines is expected to be much higher than the fourth anti–Stokes line. In Fig. 3, we have plotted the variation of intensity of the various Raman components, S_1 (λ = 416 nm), S_2 (λ = 503 nm) S_3 (λ = 636 nm), and AS_1 (λ = 309 nm) at different input laser beam energies used in the present study. It is clear from the Fig. 3 that the intensity of the S_1 and AS_1 is increasing while the intensity of the pump beam is depleting in just about the same proportion. However, the rate of growth of the S_1 wave is much higher than that of the AS_1 wave. The observation of AS_1 is most likely due to the four–wave mixing processes. Beyond 50 mJ of the pump energy, the intensity of the S_1–wave is growing strongly whereas the intensity of the S_2 and S_3 waves is decreasing.

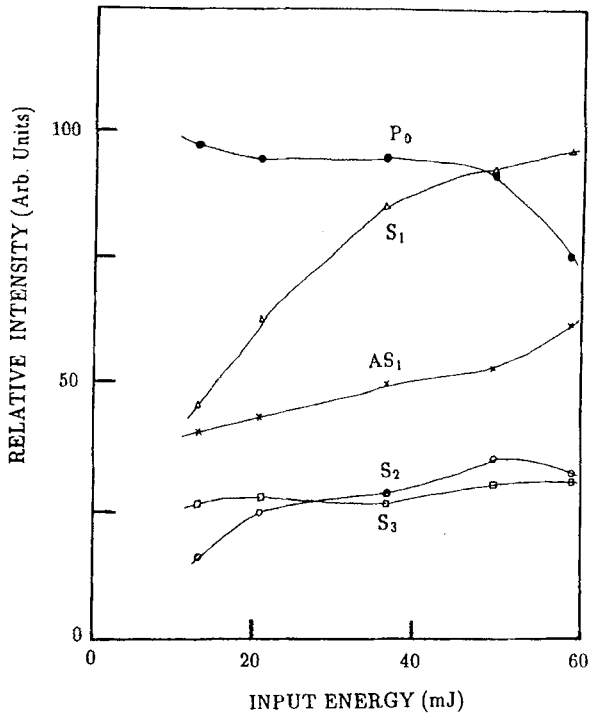

Fig. 3 The graph showing the variation of intensity of the Raman components observed in the forward direction at various input laser beam energies. The H_2–gas pressure, focal point, and the notations are the same as in Fig. 2.

The growth of the S_1 wave is consistent with the depletion of the pump laser beam intensity, which depletes drastically after 50 mJ. This observation suggests that the S_1 is being generated by the SRS–processes. The observation of higher order Raman components may be due to the four–wave mixing rather than the cascade energy transfer processes. If the cascade energy transfer processes are responsible, then one would expect formation of the S_2–wave first and then the S_3–wave and the intensity of the S_2–wave is expected to deplete while S_3–wave is growing. A close inspection of the behavior of the S_2 and S_3 Stokes lines at 13 mJ in Fig. 3 shows that the intensity of the

S_3 line is higher than that of the intensity of the S_2 line. At about 36 mJ, the intensity of the S_2 line is higher than the S_3 line and keeps going up. At about 60 mJ, the two intensities are almost equal.

B. H_2–Pressure Dependence on the SRS–processes

It is worth noting here that the energy of the pump photon, i.e., 355 nm, is $\cong$ 3.5 eV. The lowest allowed electronic level of the H_2 molecule is at $\cong$ 11.4 eV, i.e., the first electronically excited state [15] $B^1\Sigma$. Thus the Raman processes will be highly non–resonant [16] which implies a small Stimulated Raman cross–section. Therefore a large number density of the H_2–gas is required to achieve a reasonable Raman gain in the medium. In the present study, we have used the capillary tubing Raman cell to establish the pressure threshold for the observation of the first Stokes line which is germane to the formation of the high order Stokes and anti–Stokes lines. At a constant laser beam energy of 13 mJ focused to a diameter of approximately 1mm at the center of the Raman cell, 20 cm from the entrance window of the cell, the H_2–pressure threshold was determined to be about 125 PSI for the observation of the first Stokes line at λ = 416 nm. When the H_2–pressure was increased slightly, the green color appeared at λ = 503 nm. At any pressures higher than $\cong$ 150 PSI, these colors were observed to be very strong. The red color corresponding to the third Stokes line at λ = 636 nm was not observed at any H_2–pressures used here. By using the procedures described in the experimental section of this paper, we scanned and recorded the spectrum in the wavelength range of 300–644 nm at various H_2–pressures in the range of 200–500 PSI. The results are shown in Fig. 4 for a set of selected H_2–pressures at room temperature and laser pump energy of 13 mJ. The variation of intensity of the Stokes and anti–Stokes lines are given in Fig. 5 for all the H_2–pressures used in the present study. It is clear from the Fig. 4 that the first and second Stokes lines (λ = 416 nm and λ = 503 nm) and the first, second, and third anti–Stokes lines (λ = 309 nm, 274 nm, and 246 nm, respectively) were generated at the H_2–pressures used in the present study. The presence of the second order AS_1, AS_2, and AS_3–waves is the clear indication of

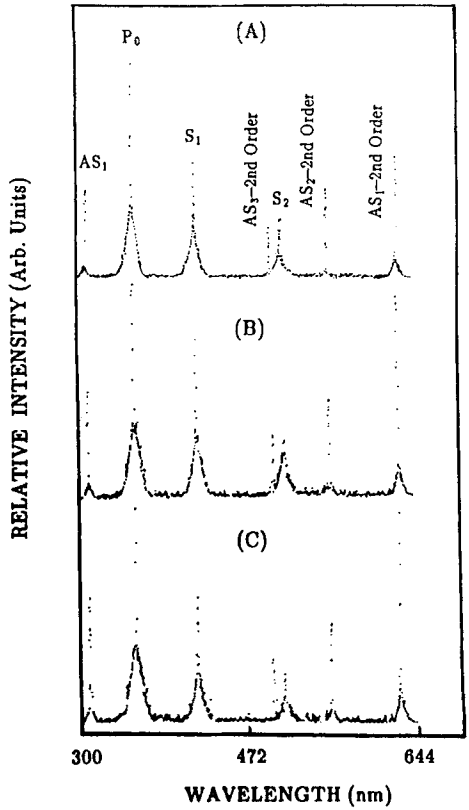

Fig. 4 Wavelength scan of the Raman components at various H_2–gas pressures at laser pump energy = 13 mJ and focal point = 20 cm. The notations are the same as in Fig. 1. The spectra are not corrected for the spectral response of the optical detection system. A:500 PSI, B:350 PSI, C:200 PSI

generation of these lines in the first order. However, there no trace of the formation of the third Stokes line at $\lambda = 636$ nm (Fig. 4). The generation of higher order components of the anti–Stokes than the Stoke lines indicates that the four–wave mixing may be the dominant mechanism for the observation of the anti–Stokes lines. From Fig. 5, it is clear that the intensity of the first Stokes, S_1, is increasing steadily and after

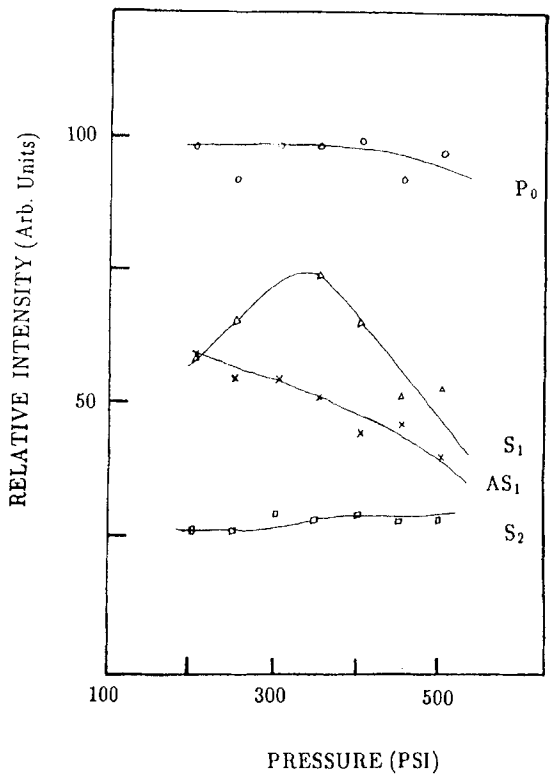

Fig. 5 The graph showing the variation of intensity of the Raman components at different H_2–gas pressures at constant pump energy, and focal point. The notations are the same as in Fig. 4.

reaching a maximum at the H_2–pressure of 350 SPI, it keeps decreasing as the pressure is increased. The intensity of the first anti–Stokes, AS_1, keeps decreasing with the increase in H_2–pressure. In relation to the intensities of S_1 and AS_1, the intensities of the second Stokes, S_2, keeps increasing with pressure at a slower rate. The formation of the S_2 may be related to the cascade energy transfer processes involving the S_1 wave.

C: Focal Length Effect on the SRS–processes:

Most of the previous studies have used long and wide bore diameter Raman cell(s) and have used a focusing lens to focus the input laser beam at the center of the cell. In the present study, using a capillary Raman cell, we have used different configurations of the focusing lens and have observed significantly different results, quite different than focusing the laser beam at the center of the cell. All the experiments were performed at H_2–gas density of 500 PSI and laser beam energy of 13 mJ. The focal length of the focusing lens, made of quartz, used here was either 50 cm or 25 cm. When the 50 cm focal length lens was placed at 2.5 cm in front of the Raman cell, the focal point was beyond the cell by 7.5 cm and no Raman scattered laser lines were observed; only the pump laser beam was evident. When the lens was moved to a distance of 13.5 cm in front of the cell, the focal point was at 36.5 cm inside the cell. In this configuration Raman lines along with the pump laser beam were observed. When the 25 cm focal length lens was placed at 5 cm in front of the Raman cell, the focal point was 20 cm inside the cell, the colors violet, green, and red were observed. At $\simeq$ 20 feet away from the dispersing prism, the spot size of these colors were of equal size and the divergence was much less than when the focal point was at 36.5 cm.

A wavelength scan indicated that the intensity of Stokes and anti–Stokes lines observed at 36.5 cm focal length was much stronger than at any other focal length configuations. At the same time, the number of Raman components observed in this configuartion were more than in any other configuarations. The enhancement in the intensity and number of higher order components may be explained based on the spontaneous Raman scattering photons, which are known to act like "seed" for the generation of the first Stokes and subsequent higher order Raman components. When the focal point is at 36.5 cm from the entrance window, the laser beam is generating more spontaneous Raman photons than when it is travelling only 5.5 cm or 20 cm inside the cell. Because of the large number of "seed" photons, one would expect the formation of an intense first Stokes line. The first Stokes will lead to the formation of other Raman components either due to the four–wave mixing or cascade energy transfer processes. It

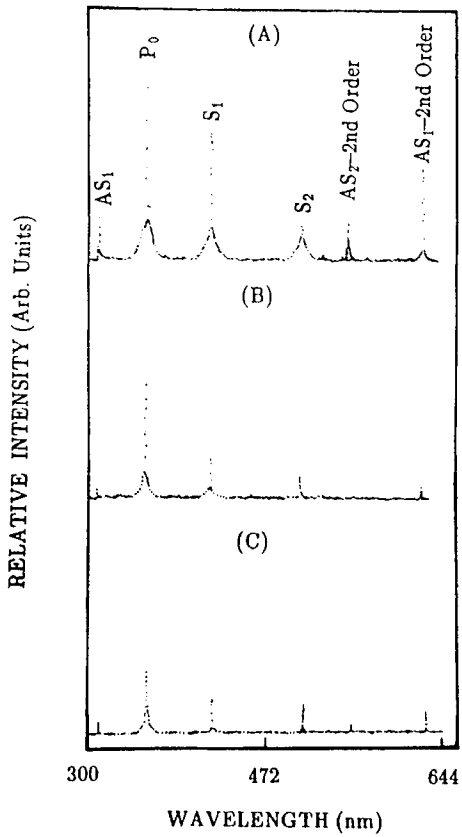

Fig. 6 Wavelength scan of the Raman components at various focal points inside the Raman cell at H_2 pressure = 500 PSI and pump energy = 13 mJ. The notations are the same as in Fig. 1. The spectra are not corrected for the spectral response of the optical detection system. A: 36.5 cm, B: 20 cm, C: 5.5 cm. The focal lengths are measured from the entrance window of the cell.

may be worth noting here that a similar observation will be expected by using a Raman cell of 2x36.5 cm, if the focal point is set at the center of the cell under the present experimental conditions. These results clearly indicate that a capillary Raman cell of 40 cm or slightly less is as good as a Raman cell of 80 cm or close to 1 meter, which has

traditionally been used in the past by many investigators. In Fig. 6, we display the wavelength scan with intensity of the Raman components at various focal points inside the Raman cell at a constant pump energy (13 mJ) and H_2–gas pressure (500 PSI).

Conclusions

In conclusion, we have studied the Stimulated Raman Scattering (SRS) processes (SRS) in H_2 gas using pulsed laser beam at wavelength $\lambda = 355$ nm. The SRS–processes were studied in a capillary Raman cell of 0.635 cm internal diameter and 40 cm long. The capillary Raman cell was found to be more efficient in generating the Raman components than a wide bore tubing of the same length. A parametric study was performed to establish the best operating condition for the Raman laser by varying the H_2 gas pressure, pump laser energy, and the focal point inside the capillary Raman cell.

ACKNOWLEDGMENTS

We gratefully acknowledge the financial support from the US Army Research Office, Grant No. DAAL–03–89–G–0099, for the research work reported here. We would like to thank Mr. A. Michael and Mr. L. Major for their help in the initial phases of the experiment. The Raman cell was fabricated jointly by Mr. E. Jones and Mr. Bill Pinkney and we are thankful to them.

REFERENCES

1. Loree, T.R., Sze, R.C., and Scott, P.B. New Lines in the UV:SRS of Excimer Laser Wavelengths. IEEE J. Quant. Elect. 1979; QE–15: 337–342.
2. Trainor, D.W., Hyman, H.A., and Heinrichs Stimulated Raman Scattering of XeF Laser Radiation in H_2. IEEE J. Quant. Elect. 1982; QE–18: 1929–1934.

3. Guntermann, G., Gathen, V., and Dobele, H.F. Raman Shifting of Nd:YAG laser Radiation in Methane: an Efficient Method to Generate 3–μm Radiation for Medical Uses. Appl. Opt. 1989; 28: 135–139.

4. Komine, H. and Stappaert, E.A. Efficient Higher Stokes–Order Raman Conversion in Molecular Gases. Opt. Lett. 1979; : 398–401.

5. Sentrayan, K., Major, L., Michael, A. and Kushawaha, V. Observation of Intense Stokes and anti–Stokes lines in CH_4 pumped by the 355 nm of Nd:YAG Laser. Appl. Phys. B (submitted, 1992).

6. Kawasaki, S., Imasaka, T., and Ishibashii, N. Two–color Stimulated Raman Effect of Para–Hydrogen. J. Opt. Soc. Am. 1991; 8: 1461–1463.

7. Trutna, W.R. and Byer, R.L. Multiple–pass Raman Gain Cell Appl. Opt. 1976; 19: 301–311.

8. McPherson, D.C., Swanson, R.C., and Carlsten, J.L. Stimulated Raman Scattering in the Visible with a Multipass Cell. IEEE J. Quant. Elect. 1989; 25: 1741–1746.

9. Schimitschek, E.J. Blue–Green Lasers. Laser Focus 1982; 18: 53–55.

10. Ancellet, G., Popayannis, A., Pelon, J., and Megie, G. DIAL Tropospheric Ozone Measurement using a Nd:YAG Laser and Raman Shifting Technique J. Atmos. Oceanol. Technol. 1989; 6: 832–839.

11. McDermid, I.S., Godin, S.M., and Lindavist, L.O. Ground Based Laser DIAL System for Long–Term Measurements of Stratospheric Ozone. Appl. Opt. 1990; 29: 2603–2612.

12. Johnston, H.S. Photochemistry in the Stratosphere: in Tunable Lasers and Applications. Ed. Mooradin, A., Jaeger, T., and Stokseth, P. Springer–Verlag, New York, 1976.

13. Grant, W., Browell, E.V., Higdon, N.S., and Ismail, S. Raman Shifting of KrF Radiation for Troposphere Ozone Measurement. Appl. Opt. 1991; 30: 2626–2633.

14. Komine, H. and Stappaert, E.A. Efficient higher–order Stokes Raman conversion in Molecular gases. Opt. Lett. 1979; 4: 398–400.

15. Herzberg, H. Molecular Spectra and Molecular Spectroscopy:Spectra of Diatomic Molecules. Vol. I, Van–Nostrand Reinhold Comp., New York, 1950

16. Nathanson, B. and Rockni, M. The Effect of Stokes and anti–Stokes coupling on the Gain of Resonant Stimulated Raman Scattering. J. Phys. D (Appl. Phys.) 1991; 24: 233–235.

Date Received: 06/19/92
Date Accepted: 07/26/92